DESIGN, IMPLEMENTATION, AND PERFORMANCE ANALYSIS OF A STEWART PLATFORM-BASED FORCE SENSOR[1]

Francesc Roure
Strength of Materials and
Structural Eng. Dept. (UPC)
Diagonal 647, 08028 Barcelona

Roger Frigola, Lluís Ros, and Federico Thomas
Institut de Robòtica i Informàtica
Industrial (UPC/CSIC)
Llorens Artigas 4-6, 08028 Barcelona

ABSTRACT

Many robotic in-parallel structures have been conceived as six-component force sensors. In general, they perform well for most applications but, when accuracy is a must, two main limitations arise. First, in most designs, the legs are connected to the base and the platform through ball-and-socket joints and the integrated effect of such elements becomes noticeable. Second, dynamical measurements might not be very accurate because the natural resonance frequency of the used structures is quite low even for relatively small dimensions. This paper discusses the development of a force sensor based on an in-parallel structure and shows how the above limitations degrade its behavior. Moreover, it shows how, using a tensegrity structure, both problems could be alleviated because ball-and-socket joints can be replaced by point contacts and the resonance frequency can be controlled by adjusting the tensions of the tendons.

Keywords: force sensor, tensegrity structure, ellipsoidal uncertainty set.

1. INTRODUCTION

The Stewart platform is a six degree-of-freedom parallel mechanism proposed by D. Stewart in 1965. Since it is an in-parallel linkage that sustains the payload in a distributive manner, it has high load capacity, and joint errors are not cumulative, as in serial manipulators. Its compact design and interesting properties have prompted different authors to consider it when designing force-torque sensors. When using a Stewart platform as a force sensor, the platform plays the role of the proof element and the sensing task consists in estimating the forces and torques acting on the platform from those measured at its legs. Legs are attached through ball-and-socket joints to guarantee that forces are only transmitted from the platform to the base along the leg lines.

The development of the first sensor of Stewart platform type is due to Gaillet and Reboulet [1]. Kerr [2] analyzed a similar structure and gave design criteria for the sensor structure. Other theoretical and experimental investigations were carried out by Sorli and Pastorelli [3]. Dasgupta et al. [4] present a design methodology for the optimal conditioning of the force transformation matrix. Svinin and Uchiyama [5] have considered the optimality of the condition number of the force transformation matrix. Dwarakanath et al. [6] report an implementation and some experimental results.

This paper presents the design, implementation and performance analysis of a Stewart platform-based force sensor. Section 2 introduces the notation and the basic mathematical background. Section 3 describes the design criteria and the implemented prototype. The experimental results, with particular emphasis on the effects of the different sources of error, are described in Section 4. Section 5 explains how the obtained accuracy could be improved by transforming the structure into a tensegrity one. The paper is concluded in Section 6 summarizing the work.

2. MATHEMATICAL BACKGROUND

Assume we have a platform in static equilibrium, connected to its environment through n legs, articulated with ball-and-socket joints (Fig. 1-left). Then, every leg applies a force $\mathbf{f}_i$ on the platform, which must be aligned with the leg and, by Poinsot's central axis theorem, any other

forces applied on the platform can be reduced to a single force $\mathbf{F}$ and torque $\mathbf{\Gamma}$ acting along the same line l. We will next see how, having sensor readings of the leg forces, we can fully recover $\mathbf{F}$, $\mathbf{\Gamma}$ and the point P where l intersects the platform. In other words, this device can be used as a force/torque sensor, and also as a tactile pad.

Let f_i and $\mathbf{e}_i$ be the force and the unit vector along leg i, respectively. The resulting wrench of leg forces, $\mathbf{w}_l \in \mathbb{R}^6$, computed with respect to a point O on the body, can be expressed as $\mathbf{w}_l = \mathbf{J} \cdot \mathbf{f}$, where $\mathbf{J}$ is a 6×6 matrix whose ith column is $\mathbf{J}_i = (\mathbf{e}_i, \mathbf{e}_i \times \mathbf{r}_i)^\top$, $\mathbf{r}_i$ is the vector from O to the ith leg attachment point, and $\mathbf{f} = (f_1, \ldots, f_n)$. Thus, if we install load cells on the legs to measure the f_i's, $\mathbf{w}_l$ can easily be determined. Moreover, if we denote by $\mathbf{w}_p$ the resulting wrench produced by $\mathbf{F}$ and $\mathbf{\Gamma}$ with respect to O, it must be $\mathbf{w}_p = (\mathbf{F}, \mathbf{F} \times (P - O) + \mathbf{\Gamma})^\top$. Since the body is in equilibrium, $\mathbf{w}_p = -\mathbf{w}_l$, and, hence, $\mathbf{F}$ is given by the first three components of $-\mathbf{w}_l$. To isolate $\mathbf{\Gamma}$ from $\mathbf{M} = \mathbf{F} \times (O - P) + \mathbf{\Gamma}$, we use the fact that $\mathbf{F}$ and $\mathbf{\Gamma}$ are aligned, i.e., $\mathbf{\Gamma} = k\mathbf{F}$, for some $k \in \mathbb{R}$. If we choose O in the origin, and let $P = (x, y, z)$, we have $\mathbf{M} = \mathbf{F} \times (x, y, z)^\top + k\mathbf{F}$. Using this equation, and assuming the X and Y axes lie on the platform, we can define a system of four linear equations in four unknowns. If l intersects the $z = 0$ plane, the system yields the unique solution

$$x = (F_1 F_2 M_1 - F_1^2 M_2 - F_3^2 M_2 + F_2 F_3 M_3)/(F_3(F_1^2 + F_2^2 + F_3^2)), \qquad (1)$$

$$y = (F_2^2 M_1 + F_3^2 M_1 - F_1 F_2 M_2 - F_1 F_3 M_3)/(F_3(F_1^2 + F_2^2 + F_3^2)), \qquad (2)$$

$$k = (F_1 M_1 + F_2 M_2 + F_3 M_3)/(F_1^2 + F_2^2 + F_3^2). \qquad (3)$$

where the F_i and M_i indicate the ith components of $\mathbf{F}$ and $\mathbf{M}$. This finally gives the coordinates of P explicitly, and allows recovering $\mathbf{\Gamma}$ as $k\mathbf{F}$.

3. THE IMPLEMENTED PROTOTYPE

If $\mathbf{F}$ and $\mathbf{\Gamma}$ can be arbitrarily oriented, then the minimum number of legs needed to compensate them is six. We could use more legs but, to get the simplest possible sensor, we adopted this number in our case. The resulting structure is thus equivalent to a Stewart platform.

Operation constraints required the platform to be circular, with a radius of 0.2 m, and able to support a maximum force of 10 N in any direction. Under these assumptions, the basic problem is how to arrange the legs so that the load they support be well-distributed among all of them. To come up with a proper design, we next see how the leg forces vary, as the external wrench $\mathbf{w}_p$ varies within a given ellipsoid of $\mathbb{R}^6$, defined by $(\mathbf{w}_p - \mathbf{w}_0)^\top \mathbf{E}_p (\mathbf{w}_p - \mathbf{w}_0) \le 1$, where $\mathbf{w}_0$ is the ellipsoid's center and $\mathbf{E}_p$ is its defining matrix. Assuming the platform's weight is negligible, the ellipsoid will be centered in the origin, and $\mathbf{E}_p$ may easily be derived from the operation constraints above. Substituting $\mathbf{w}_0 = \mathbf{0}$, and $\mathbf{w}_p = -\mathbf{J}\mathbf{f}$, yields $\mathbf{f}^\top \cdot \mathbf{J}^\top \mathbf{E}_p \mathbf{J} \cdot \mathbf{f} \le 1$, and, since $\mathbf{E}_l = \mathbf{J}^\top \mathbf{E}_p \mathbf{J}$ is positive semidefinite, this means the leg forces also take values inside an ellipsoid embedded in $\mathbb{R}^6$. This ellipsoid is centered in the origin, and its semiaxes are defined by the eigenvectors of $\mathbf{E}_l$. Note that, for all leg forces to lie on a same range, it should be $\mathbf{J}^\top \mathbf{E}_p \mathbf{J} = \mathbf{I}$. In other words, the ellipsoid should ideally be a hypersphere, and the design problem reduces to finding proper vectors $\mathbf{e}_i$ and $\mathbf{r}_i$ satisfying this criterion.

If, as required, the platform has to support 10 N in any direction, choosing O in its center yields a maximum moment of 2 Nm, meaning that $\mathbf{E}_p = \mathrm{diag}(a, a, a, b, b, b)$, with $a = 1/\sqrt{10}$ and
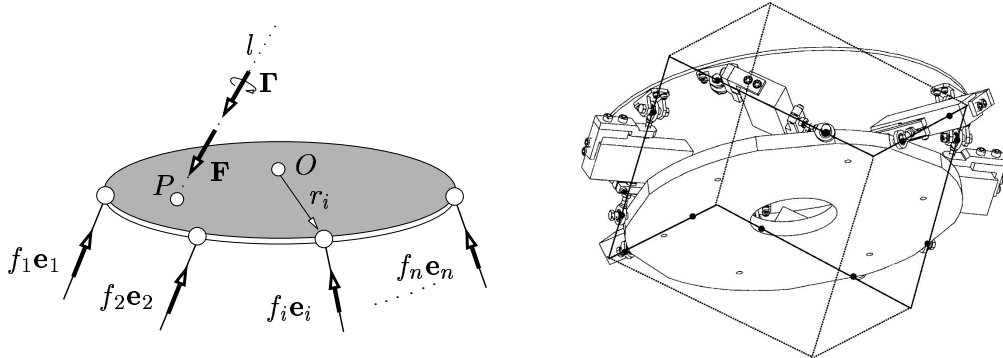

Figure 1: Left: A platform connected to its environment through n legs. Right: Conceptual design of the sensor. Legs of length 0.1 m are aligned with the edges of a cube of side 0.3 m.

Figure 2: Sensor prototype (b), details of the ball-and-socket joints (a) and the load cells (c).

$b = 1/\sqrt{2}$. One can see that, with this $\mathbf{E}_p$, and arranging the legs as depicted in Fig. 1-right, we obtain a sensor where $\mathbf{E}_l$ nearly defines a hypersphere and is hence close to optimal. Actually, this makes all leg forces lie in the interval ± 7.5 N and, thus, the installed load cells must be able to work within this range. A non-negligible platform weight just changes this interval slightly. It only shifts the ellipsoids for $\mathbf{w}_p$ and $\mathbf{f}$ away from the origin, keeping their axes' lengths. For a weight of 20 N in our case, we get an actual interval of leg forces of $[-2.4, 13.6]$ N. A low-cost load cell compatible with this range is Utilcell's 105 model, whose maximum supported force and measurement error are ± 20 N and ± 0.0039 N, respectively.

4. PERFORMANCE ANALYSIS

The main problem in the error analysis of the implemented sensor is the study of the sensibility of P's location to errors in the leg force measurements. This analysis has been carried out using ellipsoidal uncertainty sets [7]. The leg measurement error can be modelled as an ellipsoidal uncertainty set in $\mathbb{R}^6$. That is, $(\mathbf{f} - \mathbf{f}_0)^\top \mathbf{E}(\mathbf{f} - \mathbf{f}_0) \leq 1$, where the center of the ellipsoid, $\mathbf{f}_0$, is the actual measurement. Assuming that the error bounds for the six legs are the same, this ellipsoid becomes a sphere of radius λ, and $\mathbf{E} = 1/\sqrt{\lambda}\mathbf{I}$. To obtain the uncertainty in the location of the contact point, we have to propagate this ellipsoid using Eqs. (1) and (2). Since these equations cannot be expressed in the standard form $\mathbf{A}(x, y)^\top + \mathbf{C}(F_1, F_2, F_3, M_1, M_2, M_3)^\top + \mathbf{d} = \mathbf{0}$, the propagation theorem presented in [7] cannot be applied directly. We have to linearize the relationship between leg forces and contact point given by Eqs. (1) and (2). To evaluate how accurate this linearization is, we have generated random measurements inside an uncertainty ellipsoid for $\mathbf{f}$ and computed the resulting point on the platform. The result is a set of points that can always be perfectly fitted by the ellipsoid obtained using linearization, probably because errors are small and the platform is far from a singularity.

Measurement errors are not the only source of static errors. When we apply a force on the platform and we release it, we observe that the measurements do not return to their original values. The measurements in the legs are shifted up to 0.25 N in the sense induced by the force. Applying a short vibration to the platform, the measurements return to their original value. This phenomenon is due to dry friction in the ball-and-socket joints. Also, concerning dynamic errors, we have measured the forces on the six legs during periods of 300 ms, without applying any force on the platform. The force signals indicate the platform has a mechanical resonance at about 25 Hz, with an amplitude of about $0.05 N$. Besides this interference, there is background noise with a variance of about 0.006 N. These observations have been confirmed by performing a modal analysis on a finite element model of the sensor. The first five natural frequencies computed on such model are 9.973, 23.566, 23.567, 27.005, and 32.847 Hz. From an spectral analysis of the leg forces, it can be seen that only the 23.566 Hz and 23.567 Hz frequencies are relevant in practice. From the model, one sees they correspond to two identical mode shapes in the X and Y directions of the platform.

5. ELIMINATING THE BALL-AND-SOCKET JOINTS

In our prototype, legs are connected to the platform and the base through ball-and-socket joints because they can undergo both tensions and compressions during normal operation (Fig. 3a). If a leg is always in compression, its connections to the rest of the structure can be substituted by point contacts (Fig. 3b). On the contrary, if the bar is always in tension, it can be substituted
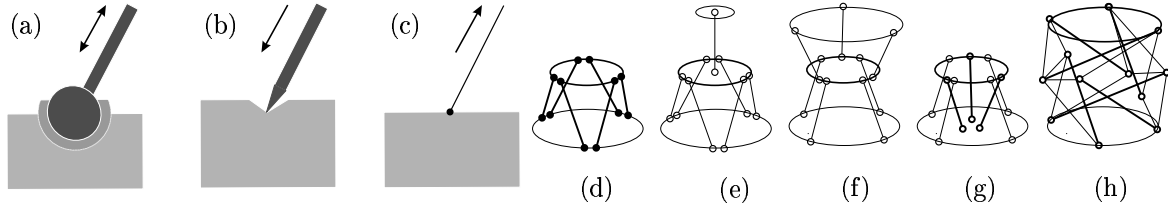
Figure 3: (a)-(c): A ball-and-socket joint can be substituted by a point contact or a tendon.(d)-(h): Thick lines correspond to rigid bars, and thin ones to elastic tendons.

by a tendon (Fig. 3c). So, the problem of eliminating the ball-and-socket joints entails finding alternative structures where all elements during normal operation are always either in tension or compression. At this point, the architectures proposed in the context of tendon-driven robots are an important source of inspiration. A parallel structure actuated by tendons requires at least seven wires to allow six degrees of freedom without involving gravity because tendons can only exert traction forces. Then, a clear evolution of our structure in which all legs are substituted by tendons in tension requires an extra tendon pulling the table upwards, as shown in Fig. 3e. Unfortunately, this structure is noticeably unbalanced (six tendons pulling on one side contrasted by only one in the other). In the structure in Fig. 3f, the tendon arrangement guarantees a better distribution of the tensions when an external wrench is applied. Now, the problem is that the access to the platform is cluttered by tendons. The solution is to substitute the tendons in tension on one side of the table by aligned bars in compression on the other, as shown in Fig. 3g so that the force equilibrium is unaltered. The resulting structure is technically known as a tensegrity structure: an assembly of bars and tendons with the ability of maintaining equilibrium with all tendons in tension in the absence of external forces [8]. Using a tensegrity structure, all ball-and-socket joints can be substituted by point contacts and, as a consequence, dry frictions can be eliminated. Another advantage of this substitution is that dynamic characteristics can be tuned by adjusting the pretension of the structure. The higher the pretension, the higher the natural frequencies. This permits adjusting the fundamental resonance frequency at will.

6. CONCLUSIONS

We have presented the design and implementation of a force/torque sensor based on a Stewart platform, and showed how two main sources of error degrade its behavior: the effect of the dry friction in the twelve ball-and-socket joints (which degrade the static measurements), and the mechanical resonance (which degrades the dynamic ones). We have concluded that a structure with a self-stress could provide a good solution to alleviate both problems, showing that structures such as those in Figs. 3g and h can be used for force/torque sensing. Our current work includes implementing a force/torque sensor based on a self-stressed structure, and extending the finite element model herein developed to tune the tendons' pretensions of the new design.

7. REFERENCES

[1] Gaillet, A., and Reboulet, C., (1983), "An Isostatic Six Component Force and Torque Sensor," *Proceedings of the 13th Int. Symposium on Industrial Robotics.*

[2] Kerr, D.R., (1989), "Analysis, Properties and Design of Stewart Platform Transducer," *Trans. ASME, J. Mech. Transm. Automn. Des.,* Vol 111, pp. 25-28.

[3] Sorli, M., and Pastorelli, S. (1995), "Six-Axis Reticulated Structure Force/Torque Sensor with Adaptable Performances," *Mechatronics,* Vol. 5, No. 6, pp. 585-601.

[4] Dasgupta, B., Reddy, S., and Mruthyunjaya, T.S., (1994), "Synthesis of a Force-Torque Sensor Based on the Stewart Platform Mechanism," *Proc. National Convention of Industrial Problems in Machines and Mechanisms* (IPROMM'94), pp. 14-23.

[5] Svinin, M.M., and Uchiyama, M., (1995) "Optimal Geometric Structures of Force/Torque Sensors," *International Journal of Robotics Research,* Vol. 14, No. 6, pp. 560-573.

[6] Dwarakanath, T.A., Dasgupta, B., Mruthyunjaya, T.S. (2001), "Design and Development of a Stewart Platform Based Force-Torque Sensor," *Mechatronics,* Vol. 11, No. 7, pp. 793-809.

[7] Ros, L., Sabater, A., and Thomas, F. (2004), "An Ellipsoidal Calculus Based on Propagation and Fusion," *IEEE Trans. on Syst., Man, and Cyb. - Part B: Cybernetics,* Vol. 32, No. 4, pp. 430-442.

[8] R. Motro (2003), *Tensegrity. Structural Systems for the Futures,* Kogan Page Science, London and Sterling, VA, 2003.